CHEMISTRY OF MATERIALS
Communication

Chem. Mater. **2010,** *22,* 3829–3831 3829
DOI:10.1021/cm101217k

Hollow Carved Single-Crystal Mesoporous Silica Templated by Mesomorphous Polyelectrolyte−Surfactant Complexes

Jin-Gui Wang, Hui-Jing Zhou, Ping-Chuan Sun, Da-Tong Ding, and Tie-Hong Chen*

Institute of New Catalytic Materials Science, Key Laboratory of Advanced Energy Materials Chemistry (MOE), College of Chemistry, Nankai University, Weijin Road 94, Tianjin 300071, China

Received February 26, 2010
Revised Manuscript Received May 30, 2010

One amazing feature in biomineralization is that some biominerals, such as the sea-urchin spines, exhibit complex and spongelike morphology but still remain a single crystal.[1] The remarkable "fabrication skill" of nature greatly inspires the study on preparation of single crystalline materials with complex morphologies, and porous/nanostructured calcite single crystals were fabricated.[2] The deposition of biominerals is generally controlled by specific organic matrix secreted and transferred by the organisms, and the formation process of the hierarchical biominerals is controlled by a time-dependent cooperative organization, in which organic matrix acts as dynamic template.[3] Though dynamic templating processes prevail in biomineralization, there are few examples reported of the fabrication of hierarchically structured materials.[4] Herein, by using mesomorphous polyelectrolyte−surfactant complexes as dynamic template, we report for the first time the fabrication of hierarchically nanoporous single-crystal mesoporous silica SBA-1.

Ionic self-assembly of polyelectrolyte and oppositely charged surfactants can form highly ordered mesomorphous liquid crystalline phases and is a versatile tool to create supramolecular materials.[5] Mesoporous materials are generally synthesized by self-assembly of organic and inorganic species, however, the organic mesomorphous complexes were rarely utilized to control the mesostructure and morphology of mesoporous materials.[6] Though anionic polymers were used in cationic surfactant-templated mesoporous silica, they were added either in acidic condition to avoid complexation with the surfactants[7]or in mixed solvents to form a homogeneous solution,[8] or the molecular weight of anionic polymer was relatively low and formation of the mesomorphous polyelectrolyte−surfactant complexes was not identified.[9]

In this work, anionic polymer poly(acrylic acid) (PAA) was used to complex with cationic surfactant cetyltrimethylammonium bromide (CTAB) in ammonia solution (see the Supporting Information) and dispersed submicrometer organic complex particles were formed (see Figure S1 in the Supporting Information). The solidlike PAA-cetyltrimethylammonium(C_{16}TA) organic complex exhibited ordered cubic ($Pm\bar{3}n$) or mixed mesomorphous phases depending on the amount of ammonia (see Figure S2 in the Supporting Information). To this suspension solution of PAA-C_{16}TA complex particles, TEOS was added as inorganic species to coassembly with the complex template to form silica-based mesostructured materials.

The small-angle X-ray scattering (SAXS) patterns of the as-synthesized (see Figure S3 in the Supporting Information) and calcined (Figure 1) silica samples synthesized at different temperature (see Table S1 in the Supporting Information) indicated three distinct diffraction peaks indexed to (200), (210), and (211) diffractions respectively, according to the cubic $Pm\bar{3}n$ mesostructure. SEM images showed that the samples were generally submicrometer spherical particles (Figure 2a and Figure S4 in the Supporting Information). The surface of the spheres was not smooth and exhibited a furrow or sulcus-like morphology (Figure 2a). TEM mages showed different contrast inside the microspheres (Figure 2b), implying the presence of interstitial pores (as was proved by nitrogen adsorption discussed below). The interstitial pores in the calcined samples were more obvious than that in the as-synthesized samples observed from the TEM images (see Figures S5 and S6 in the Supporting Information). The representative high-resolution TEM images (Figure 2c,d) of the microspheres confirmed the different contrast inside the microsphere. What amazing was that the whole particle was a hollow carved single crystal with $Pm\bar{3}n$ mesostructure. As shown in Figure 2c, the cagelike mesopores kept well long-range order within the whole particle along the [100] direction in spite of the presence of interstitial nanopores. The TEM images were obtained with the whole particles while not sliced sample and only the particles whose crystal orientation was aligned along the incident electron beam could be observed with clear mesostructured fringes and cages. It should be noted that the Fourier

*Corresponding author. E-mail: chenth@nankai.edu.cn.

(1) Meldrum, F. C.; Colfen, H. *Chem. Rev.* **2008**, *108*, 4332.
(2) (a) Li, C.; Qi, L. *Angew. Chem., Int. Ed.* **2008**, *47*, 2388. (b) Finnemore, A.; Scherer, M.; Langford, R.; Mahajan, S.; Ludwigs, S.; Meldrum, F.; Steiner, U. *Adv. Mater.* **2009**, *21*, 3928. (c) Li, C.; Qi, L. *Adv. Mater.* **2010**, *22*, 1494.
(3) Mann, S. *Biomineralization: Principles and Concepts in Bioinorganic Materials Chemistry*; Oxford University Press: New York, 2001.
(4) (a) Pouget, E.; Dujardin, E.; Cavalier, A.; Moreac, A.; Valery, C.; Marchi-Artzner, V.; Weiss, T.; Renault, A.; Paternostre, M.; Artzner, F. *Nat. Mater.* **2007**, *6*, 434. (b) Brunner, E. *Nat. Mater.* **2007**, *6*, 398.
(5) (a) Antonietti, M.; Conrad, J. *Angew. Chem., Int. Ed.* **1994**, *33*, 1869. (b) Faul, C.; Antonietti, M. *Adv. Mater.* **2003**, *15*, 673. (c) Piculell, L.; Norrman, J.; Svensson, A.; Lynch, I.; Bernardes, J.; Loh, W. *Adv. Colloid Inter. Sci.* **2009**, *147−148*, 228. (d) Ikkala, O.; Brink, G. *Science* **2002**, *295*, 2407.
(6) Yang, B.; Edler, K. *Chem. Mater.* **2009**, *21*, 1221.
(7) (a) Pantazis, C.; Pomonis, P. *Chem. Mater.* **2003**, *15*, 2299. (b) Rathod, S.; Ward, T. *J. Mater. Chem.* **2007**, *17*, 2329.
(8) Guo, X.; Deng, Y.; Tu, B.; Zhao, D. *Langmuir* **2010**, *26*, 702.
(9) Peng, J.; Na, H.; Lu, Y. *Microporous Mesoporous Mater.* **2005**, *86*, 89.

Published on Web 06/11/2010

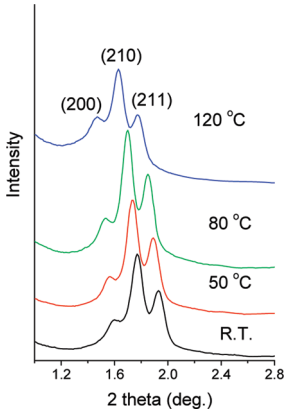

Figure 1. SAXS patterns of the calcined SBA-1 samples prepared at (a) RT (20−25 °C), (b) 50 °C, (c) 80 °C, and (d) 120 °C.

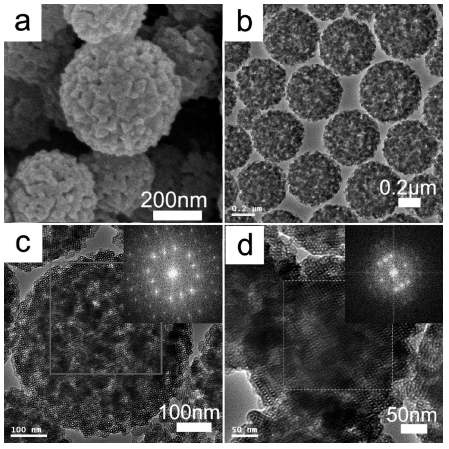

Figure 2. (a) SEM and (b−d) TEM images and their Fourier diffractograms (insets) of the calcined SBA-1 spheres synthesized at 120 °C. The TEM images were recorded along the direction of (c) [100] and (d) [210].

diffractograms (insets in Figure 2) were obtained from the area of several hundreds of nanometers. Other TEM images (Figure S7) of the microspheres synthesized at different temperature also displayed the character of single crystal SBA-1 along different directions. To the best of our knowledge, this is the first fabrication of single crystal mesoporous silica with interstitial nanopores (secondary nanopores).

The nitrogen adsorption−desorption isotherms of the SBA-1 spheres synthesized at different temperature were shown in Figure 3. Samples synthesized at room temperature and 50 °C exhibited type IV isotherms with three distinct adsorption steps at the relative pressure of 0.3−0.5, 0.7−0.95, and 0.95−0.99, respectively. The first step corresponded to the relatively narrow peaks at about 3 nm in the pore size distribution curves, which were the pore size of the mesoporous SBA-1. It is necessary to indicate that the SBA-1 has an ordered 3D mesostructure with two types of globular cages, which possess slightly different pore sizes.[10] The peak at about 3 nm was due to the overlap of the two types of globular cage-like mesopores. The second adsorption step gave rise to a broad pore size centered at ∼20 nm

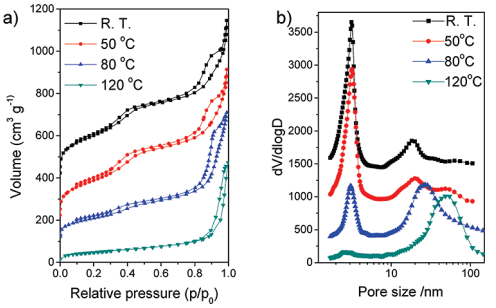

Figure 3. (a) Nitrogen adsorption−desorption isotherms and (b) PSD curves of the calcined samples synthesized at different temperatures. The lines were shifted upward for clarity.

corresponding to the secondary interstitial nanopores observed in the TEM images. The third adsorption step was due to the voids of the aggregated submicrometer spheres, and probably some larger secondary nanopores inside the single-crystal SBA-1 particles could also contribute to the third adsorption step. Samples synthesized at 80 and 120 °C exhibited type IV isotherms with two distinct adsorption steps at the relative pressure of 0.3−0.5 and 0.7−0.99, respectively. In the pore size distribution curves, the first step also corresponded to the nitrogen capillary condensation in the cagelike pores of the mesoporous SBA-1. The second adsorption step was mainly due to the interstitial nanopores as observed in TEM images and the average pore size was increased to ∼30 and ∼50 nm, respectively. The adsorption step corresponding to the large interstitial nanopores also overlapped with that corresponding to the aggregated voids of the particles.

We also performed syntheses with different amounts of PAA. It was found that with the increase in PAA the average size of the PAA-C_{16}TA organic complex particles also increased (see Figure S8 in the Supporting Information). SBA-1 spheres could be obtained at different amount of PAA (see Figure S9 in the Supporting Information) and the average size of the SBA-1 spheres enlarged with the increase of PAA (see Figure S10 in the Supporting Information). This implied that the size of the silica spheres was correlative with the size of the PAA-C_{16}TA complex particles. The pore size of the secondary nanopores also increased when more PAA was used in the synthesis (see Figure S11 in the Supporting Information).

Time-dependent experiment showed that the formation process of SBA-1 sphere was very fast, which was consistent with the reported results about cationic surfactant templating mesoporous silica.[11] After stirring the reactant mixture at room temperature for 15 min, submicrometer spherical particles with ordered mesostructure ($Pm\bar{3}n$) had already formed (see Figures S12 and S13 in the Supporting Information). After subsequent reaction at 80 °C, the mesostructure order and the cross-linking degree of the silica increased with the reaction time (see Figures S13 and S14 in the Supporting Information). Nitrogen adsorption characterization showed that the average size of the secondary nanopores slightly increased with reaction time

(10) (a) Huo, Q.; Margolese, D. I.; Ciesla, U.; Feng, P.; Gier, T. E.; Sieger, P.; Leon, R.; Petroff, P. M.; Schuth, F.; Stucky, G. D. *Nature* **1994**, *368*, 317. (b) Huo, Q.; Leon, R.; Petroff, P. M.; Stucky, G. D. *Science* **1995**, *268*, 1324.

(11) (a) Tan, B.; Rankin, S. E.. *J. Phys. Chem. B* **2004**, *108*, 20122. (b) Nakamura, T.; Mizutani, M.; Nozaki, H.; Suzuki, N.; Yano, K. *J. Phys. Chem. C* **2007**, *11*, 1093.

Scheme 1. Schematic Illustration of the Formation of PAA-C_{16}TA Mesomorphous Complexes and the Dynamic Formation Process of SBA-1 Single Crystal with Secondary Nanopores

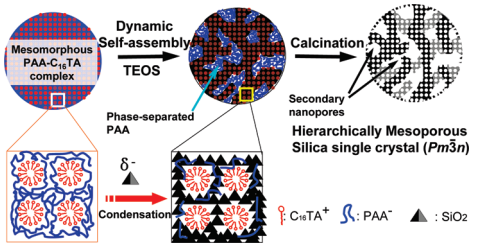

(see Figure S15 in the Supporting Information). Thermogravimetric analysis (see Figure S16 in the Supporting Information) showed that the weight loss of the organic components slightly decreased with the reaction time, because of the increasing silica condensation with time; however, the decomposition of PAA and CTAB could not be separated. ^{13}C CP/MAS NMR spectrum (see Figure S17 in the Supporting Information) of the as-synthesized product confirm that the presence of the both the PAA and C_{16}TA in the final mesostructured silica.

On the basis of the above results and time-dependent experiment, a tentative mechanism was proposed to illustrate the formation of hierarchically nanoporous SBA-1 single-crystal spheres (Scheme 1). The co-organization of PAA and CTA micelles resulted in the ordered mesophase and spherical mesomorphous PAA-C_{16}TA complex was first formed and suspended in the solution. Upon adding the silica precursor (TEOS) to the suspension of mesomorphous PAA-C_{16}TA complex, the hydrolysis of the silica precursors triggers the reassembly of the organic/inorganic species and the negatively charged silica oligomers (at pH 10−11) participated in the co-organization with the mesomorphous PAA-C_{16}TA complexes. The electrostatic interactions between PAA and C_{16}TA were disturbed by the guest negatively charged silica oligomers. The inorganic species penetrated the ordered mesomorphous complexes and cross-linked around the orderly packed cationic micelles to form the mesostructured silica of SBA-1. Meanwhile the electrostatic interactions between PAA chains and the surfactants were perturbed or disassembled and some PAA chains were disassociated from the complexes to form phase-separated PAA chain domains (with ammonium cations as the charge counterparts). The phase-separated PAA could serve as the templates for the interstitial nanopores inside the SBA-1 spheres after calcination. On one hand, the mesomorphous PAA/C_{16}TA complex first induced the mesostructure of the silica, on the other hand, because of the coassembly of the silica precursors, the PAA was phase-separated from the original complex template. In this respect, the mesomorphous PAA/C_{16}TA complexes could be regarded as a dynamic template instead of a static template during the formation of hierarchically nanoporous single-crystal SBA-1.

The silica samples prepared at different temperatures, with different amounts of PAA, or for different reaction times exhibited cubic $Pm\bar{3}n$ mesostructure; however, the mesophase of the PAA/C_{16}TA complex was not necessarily the same as that of the silica (Figures S2 and S18 in the Supporting Information). With the addition of silica precursors, the organic−inorganic coassembly would induce realignment or phase transition of the PAA/C_{16}TA complex mesophase, although not a simple replication or solidification process of the preformed polyelectrolyte−surfactant mesophase. However, the accordant mesophase through the whole PAA/C_{16}TA complex particle would induce the same alignment of the mesostructure within the hybrid particle. Through the synergy of two coupled kinetic self-assembly processes of silica−surfactants, coassembly and PAA phase separation, the mesophase through the whole PAA/C_{16}TA particle was inherited and evolved into single-crystal SBA-1 sphere with domains of phase-separated PAA chains.

Concerning the as-synthesized and calcined SBA-1 samples synthesized at different temperature, the d_{210} spacing value gradually increased with the reaction temperature (see Table S1 in the Supporting Information). Higher reaction temperature would increase the condensation rate and the cross-link degree of the silica, and this would increase the mesopore wall thickness as well as the lattice parameter of the mesostructure. The decreasing pore size with the increasing reaction temperature implied that the narrower mesopore was templated by the PAA/C_{16}TA complex micelles instead of the CTAB micelles alone. Increasing reaction temperature would facilitate the interaction between silica precursors and CTAB, and thus silica oligomers would replace more PAA chains from the complex micelles and thus the pore size became smaller. A larger amount of the disassociated PAA chains would give rise to a larger domain size and thus resulted in larger secondary nanopores after calcination (see Table S1 in the Supporting Information). When the reaction temperature was increased from room temperature to 120 °C, the lattice parameter ($a_0 = \sqrt{5}d_{210}$) of the $Pm\bar{3}n$ mesostructure increased and the pore size decreased. This implied that the thickness of the mesopore walls increased and so the porosity of the mesoporous silica was reduced. This could explain the decreasing BET surface area and mesopore volume with increasing of the reaction temperature.

In summary, hollow carved single-crystal mesoporous silica was fabricated with mesomorphous polyelectrolyte−surfactant complexes as dynamic template. The dynamic templating mechanism would be generally applicable in the fabrication of other hierarchically structured materials. Interestingly and importantly, the presence of a large amount of secondary nanopores did not disturb the single-crystal mesostructure of the mesoporous silica particles, which would possess both the functions of crystal-like regularity and high diffusion efficiency of hierarchical pores.

Acknowledgment. This work was supported by National Science Foundation of China (Grants 20873070, 20973095), National Basic Research Program of China (2009CB623502), and Ministry of Education (NCET-07-0448).

Supporting Information Available: Experimental procedure, SEM images, TEM images, and SAXS patterns (PDF). This material is available free of charge via the Internet at http://pubs.acs.org.